

The crystal and molecular structures of the nickel(II) complexes of malonamide-derived unsubstituted 14- and 13-membered tetraazamacrocycles and NMR study of the complexes in aqueous solution †

Yaroslav D. Lampeka,^{*a} Sergey P. Gavrish,^a (the late) Robert W. Hay,^b Tanja Eisenblätter^b and Philip Lightfoot^b

^a L. V. Pisarzhevskii Institute of Physical Chemistry, National Academy of Sciences of Ukraine, Prospekt Nauki 31, Kiev 03039, Ukraine. E-mail: ditop@iphch.kiev.ua

^b School of Chemistry, University of St Andrews, St Andrews, Fife, UK KY16 9ST

Received 24th February 2000, Accepted 8th May 2000

Published on the Web 13th June 2000

The crystal structures of the nickel(II) complexes of the 14- and 13-membered malonamide-derived macrocycles $[\text{NiL}^1] \cdot 6\text{H}_2\text{O}$ and $[\text{NiL}^2] \cdot 5\text{H}_2\text{O}$ ($\text{H}_2\text{L}^1 = 1,4,8,11$ -tetraazacyclotetradecane-5,7-dione, $\text{H}_2\text{L}^2 = 1,4,7,10$ -tetraazacyclotridecane-11,13-dione) have been determined. Two deprotonated amide and two amine donors form the approximately square planar environment of the metal in both complexes. The averaged $\text{Ni}-\text{N}_{\text{amide}}$ and $\text{Ni}-\text{N}_{\text{amine}}$ bonds are longer in the complex of the 14-membered macrocycle as compared to the 13-membered one (1.889 vs. 1.839 Å and 1.941 vs. 1.889 Å for $[\text{NiL}^1]$ and $[\text{NiL}^2]$ respectively). Water molecules do not co-ordinate but form an extended network of hydrogen bonds in the crystal lattices. The ligand in $[\text{NiL}^1] \cdot 6\text{H}_2\text{O}$ has the *N-meso* and in $[\text{NiL}^2] \cdot 5\text{H}_2\text{O}$ the *N-rac* configuration of the secondary amino groups. The analysis of ^1H NMR spectra reveals that the solid state conformation of both the 14- and 13-membered co-ordinated ligands is retained in aqueous solution though a substantial amount of the *N-meso* isomer is also detected for the latter.

Introduction

The co-ordination chemistry of azamacrocyclic ligands containing amide donor groups has received much attention in recent years. Such compounds have the structural features of both macrocyclic amines and oligopeptides and display many interesting properties and functions, serving as effective ligands with respect to early and late transition metals.^{1–6} In addition, they show an ability for the stabilisation of high oxidation states of metals such as nickel(III) and copper(III).^{1,2b,3a,4,6–8} Among these compounds malonamide derived macrocycles readily accessible *via* the aminolysis reactions of malonic esters with open-chain polyamines⁸ have been studied most extensively. Since the pioneering work of Kodama and Kimura⁹ the structures of a number of the nickel complexes with *N*- or *C*-substituted 13- and 14-membered macrocyclic malonamides have been determined.¹⁰ However, the structures of the complexes of the “basic” unsubstituted 14- and 13-membered dioxotetraamines H_2L^1 and H_2L^2 (see Chart 1) have not been reported to date. Moreover, in spite of the diamagnetism of nickel complexes with these ligands no detailed analysis of their ^1H NMR spectra has been presented in the literature. It is evident that, on the one hand, the availability of both X-ray structural data and accurate NMR parameters is necessary for the development of approaches to access the solution structure of metal complexes and on the other is very important from the comparative point of view for the elucidation of the influence of ligand structural variations on the properties of co-ordination compounds.

Therefore, the present paper addresses the peculiarities of the structures of the nickel complexes of 14- and 13-membered

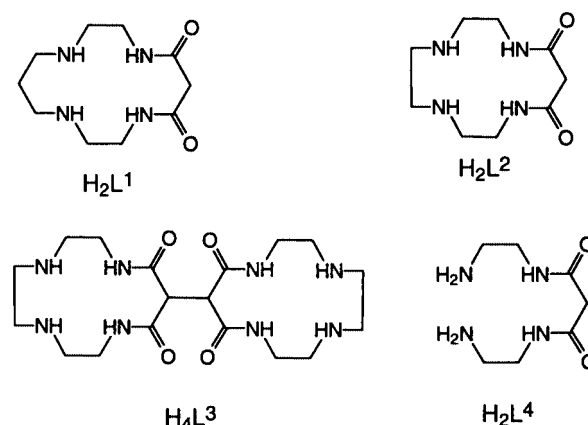


Chart 1

ligands $[\text{NiL}^1] \cdot 6\text{H}_2\text{O}$ and $[\text{NiL}^2] \cdot 5\text{H}_2\text{O}$ in comparison with the binuclear complex $[\text{Ni}_2\text{L}^3] \cdot 6\text{H}_2\text{O}$ ¹¹ and open-chain analogue $[\text{NiL}^4] \cdot 3\text{H}_2\text{O}$ ¹² whose structures have been described formerly. In order to elucidate the solution structures of the compounds under consideration and to compare them with those in the solid state, detailed analysis of ^1H NMR spectra of $[\text{NiL}^1]$ and $[\text{NiL}^2]$ in aqueous solution was carried out.

Experimental

Syntheses

The ligands H_2L^1 (1,4,8,11-tetraazacyclotetradecane-5,7-dione) and H_2L^2 (1,4,7,10-tetraazacyclotridecane-11,13-dione) and their nickel(II) complexes were prepared as previously described.¹³ Single crystals of $[\text{NiL}^1] \cdot 6\text{H}_2\text{O}$ and $[\text{NiL}^2] \cdot 5\text{H}_2\text{O}$ suitable for X-ray analysis were grown by slow diffusion of acetonitrile into aqueous solutions of the complexes.

† Supplementary data available: mean plane geometries, 2-D ^1H NMR spectra for complexes. Available from BLDSC (SUPP. NO. 57706, 5 pp.). See Instructions for Authors, Issue 1 (<http://www.rsc.org/dalton>).

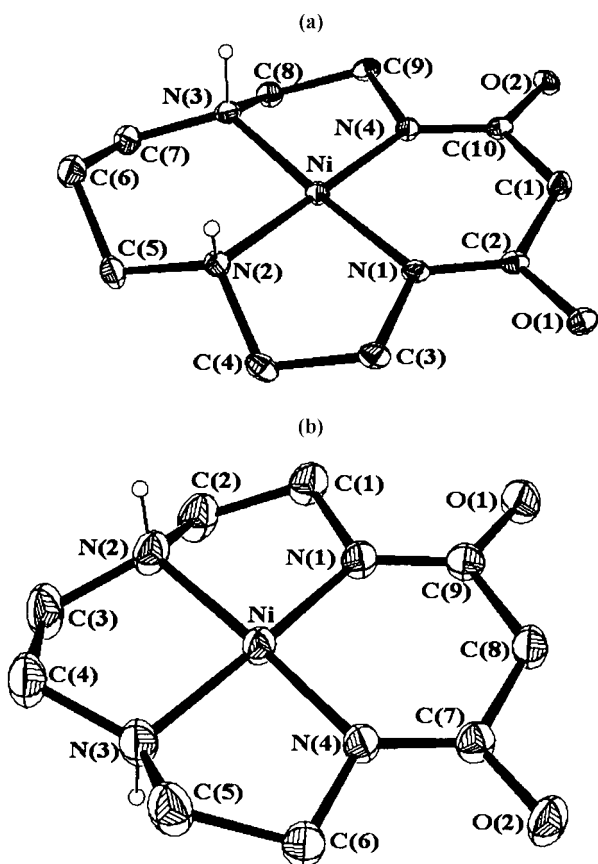


Fig. 1 Perspective views of complex $[\text{NiL}^1]$ (a) and $[\text{NiL}^2]$ (b) with the atom numbering schemes. Thermal ellipsoids are drawn at the 30% probability level; the lattice water molecules are not represented.

X-Ray crystallography

Measurements were made on a Rigaku AFC7S diffractometer with graphite monochromated Mo-K α radiation. The data were collected using the ω - 2θ scan technique to a maximum 2θ value of 50.0° . The intensities were corrected for Lorentz, polarisation and absorption effects. Other crystal data and experimental parameters are summarised in Table 1. The structures were solved by direct methods¹⁴ and expanded by Fourier techniques. The non-hydrogen atoms were refined anisotropically. Hydrogen atoms attached to C and N were placed geometrically and treated as riding atoms; those of water molecules were located by Fourier methods and refined isotropically. All calculations were carried out using the TEXSAN crystallographic software package.¹⁵

CCDC reference number 186/1973.

See <http://www.rsc.org/suppdata/dt/b0/b001510p/> for crystallographic files in .cif format.

NMR studies

The ^1H NMR spectra of complexes in D_2O solution were measured at 303 K on a Varian 500 MHz spectrometer and referenced to the solvent signal (δ 4.720). The spectra were simulated with gNMR 3.6 software.¹⁶

Results and discussion

Crystal and molecular structures of $[\text{NiL}^1]\cdot 6\text{H}_2\text{O}$ and $[\text{NiL}^2]\cdot 5\text{H}_2\text{O}$

The crystal lattices of the complexes consist of the neutral macrocyclic units and water molecules involved in a network of hydrogen bonds. The geometry of the macrocyclic compounds with atom numbering scheme applied is shown in Fig. 1. Bond distances and selected bond angles are listed in Tables 2 and 3.

Table 1 Crystal data for $[\text{NiL}^1]\cdot 6\text{H}_2\text{O}$ and $[\text{NiL}^2]\cdot 5\text{H}_2\text{O}$

	$[\text{NiL}^1]\cdot 6\text{H}_2\text{O}$	$[\text{NiL}^2]\cdot 5\text{H}_2\text{O}$
Chemical formula	$\text{C}_{10}\text{H}_{30}\text{N}_4\text{NiO}_8$	$\text{C}_9\text{H}_{26}\text{N}_4\text{NiO}_7$
Formula weight	393.07	361.03
Crystal system	Monoclinic	Triclinic
Space group	$P2_1/n$ (no. 14)	$P\bar{1}$ (no. 2)
$a/\text{\AA}$	7.247(2)	9.892(3)
$b/\text{\AA}$	24.982(4)	11.279(4)
$c/\text{\AA}$	9.436(3)	7.352(2)
$\alpha/^\circ$		94.48(2)
$\beta/^\circ$	92.17(3)	102.43(2)
$\gamma/^\circ$		83.95(3)
$V (\text{\AA}^3)$	1707.1(7)	795.3(4)
T/K	200(1)	293(1)
Z	4	2
$\mu(\text{Mo-K}\alpha)/\text{cm}^{-1}$	11.82	12.56
No. reflections measured	Total 3141, unique 2288	Total 2976, unique 2797
R_{int}	0.039	0.026
R	0.048	0.041
R_w	0.054	0.040

Table 2 Selected interatomic distances (\AA) and angles ($^\circ$) for $[\text{NiL}^1]\cdot 6\text{H}_2\text{O}$ with estimated standard deviations (e.s.d.s) in parentheses

Nickel environment			
Ni–N(1)	1.895(4)	Ni–N(2)	1.947(4)
Ni–N(3)	1.935(4)	Ni–N(4)	1.882(4)
N(1)–Ni–N(2)	85.0(2)	N(1)–Ni–N(3)	176.2(2)
N(1)–Ni–N(4)	94.1(2)	N(2)–Ni–N(3)	95.9(2)
N(2)–Ni–N(4)	177.8(2)	N(3)–Ni–N(4)	84.8(2)
Ligand			
N(1)–C(2)	1.302(7)	N(4)–C(10)	1.308(7)
O(1)–C(2)	1.294(6)	O(2)–C(10)	1.277(6)
O(1)–C(2)–N(1)	123.2(5)	O(1)–C(2)–C(1)	115.2(5)
N(1)–C(2)–C(1)	121.6(5)	O(2)–C(10)–N(4)	124.3(5)
O(2)–C(10)–C(1)	115.3(5)	N(4)–C(10)–C(1)	120.4(5)
Torsion angles			
Ni–N(1)–C(2)–O(1)	175.7(4)	Ni–N(1)–C(2)–C(1)	–3.7(8)
Ni–N(4)–C(10)–O(2)	–178.0(4)	Ni–N(4)–C(10)–C(1)	0.9(8)
N(1)–C(3)–C(4)–N(2)	–40.8(6)	N(3)–C(8)–C(9)–N(4)	38.9(6)

Table 3 Selected interatomic distances (\AA) and angles ($^\circ$) for $[\text{NiL}^2]\cdot 5\text{H}_2\text{O}$ with e.s.d.s. in parentheses

Nickel environment			
Ni–N(1)	1.838(3)	Ni–N(2)	1.890(3)
Ni–N(3)	1.885(3)	Ni–N(4)	1.840(3)
N(1)–Ni–N(2)	87.4(1)	N(1)–Ni–N(3)	171.1(1)
N(1)–Ni–N(4)	98.2(1)	N(2)–Ni–N(3)	87.8(1)
N(2)–Ni–N(4)	173.1(1)	N(3)–Ni–N(4)	87.1(1)
Ligand			
N(1)–C(9)	1.309(4)	N(4)–C(7)	1.304(4)
O(1)–C(9)	1.267(4)	O(2)–C(7)	1.266(4)
O(2)–C(7)–N(4)	124.0(3)	O(2)–C(7)–C(8)	116.1(3)
N(4)–C(7)–C(8)	119.9(3)	O(1)–C(9)–N(1)	124.1(3)
O(1)–C(9)–C(8)	116.1(3)	N(1)–C(9)–C(8)	119.8(3)
Torsion angles			
Ni–N(1)–C(9)–O(1)	–177.7(3)	Ni–N(1)–C(9)–C(8)	2.3(5)
Ni–N(4)–C(7)–O(2)	–177.5(3)	Ni–N(4)–C(7)–C(8)	4.0(5)
N(1)–C(1)–C(2)–N(2)	40.5(4)	N(2)–C(3)–C(4)–N(3)	–49.0(4)
N(3)–C(5)–C(6)–N(4)	37.7(4)		

The co-ordination polyhedra of the nickel(II) in both complexes are formed by two deprotonated amide and two amine nitrogen atoms surrounding the metal in a nearly square-planar

manner. In both complexes the nitrogen atoms deviate slightly from the mean N_4 plane with larger deviation in the 13- (r.m.s. 0.10 Å) as compared to the 14-membered compound (0.01 Å) or the open-chain analogue $[NiL^4]$ (0.04 Å).¹² In contrast to the latter, where the metal atom lies in a N_4 plane, in the two macrocyclic complexes it is shifted from this plane by 0.05 $[NiL^1]$ and 0.02 Å $[NiL^2]$.

The average distance to the deprotonated amide groups ($Ni-N_{amide}$) in $[NiL^1]$ (1.889 Å) and $[NiL^4]$ (1.869 Å) is longer than in $[NiL^2]$ (1.839 Å). Analogously, the nickel–amine donor bonds ($Ni-N_{amine}$) are the shortest in the complex of the 13-membered macrocycle (1.889 Å) and the longest in the 14-membered derivative (1.941 Å) with an intermediate value (1.921 Å) for the open-chain compound.¹² Interestingly, in all cases the difference between $Ni-N_{amine}$ and $Ni-N_{amide}$ bond lengths is nearly constant (0.05 Å). Owing to the higher conformational flexibility of the open-chain ligand, its complex can be considered as the least strained system. Therefore, the lengthening of the $Ni-N$ distances in NiL^1 as compared to NiL^4 can be considered as an indication that the aperture of the 14-membered macrocycle is somewhat too large for the accommodation of a low-spin nickel(II) ion in a square planar manner.

Deprotonation of the amide groups caused by the coordination of metal leads to the enhancement of electron delocalisation in amide fragments which become planar (the sum of the angles around the amide carbon is close to 360°, Tables 2 and 3). This also results in the lengthening of C–O and shortening of C–N distances in the complexes as compared to unco-ordinated ligands (*cf.* 1.230 and 1.335 and 1.224 and 1.331 Å for metal-free H_2L^1 and H_2L^2 respectively^{17,18} with those for $[NiL^1]$ and $[NiL^2]$).

The 6-membered trimethylenediamine chelate ring in $[NiL^1]$ possesses the typical chair conformation. The malonamide metalocycles adopt a flattened boat conformation (half-boat). For the complexes under consideration they are nearly planar in the $C_{methylene}$ part while the deviation of the nickel atom from a N_2C_2 mean plane becomes smaller in the sequence $[NiL^4]$ (0.23), $[NiL^1]$ (0.16), $[NiL^2]$ (0.03 Å). Notably, the presence of the substituent at the $C_{methylene}$ atom leads to much larger deviation of $C_{methylene}$ as well as nickel atoms from the C_2N_2 plane.^{10b,11,19}

The lateral 5-membered chelate rings in all complexes are in envelope conformation. Both carbon atoms in these rings are located on the same side of a $N_{amide}NiN_{amine}$ plane with larger displacement of the atoms connected to amine nitrogens (see Supplementary Table S1). The additional 5-membered chelate ring in $[NiL^2]$ possesses a *gauche* conformation. It is worthwhile to note that in the parent bismacrocyclic dinickel complex $[Ni_2L^3]$ this chelate ring adopts the envelope geometry (see Table S1).¹¹

As follows from the structural data, the lateral 5-membered rings in $[NiL^1]$ possess opposite chirality ($\delta\lambda$) thus this complex is the NH-*meso* isomer. In contrast, the 13-membered ligand in $[NiL^2]$ possesses a $\delta\delta$ combination of 5-membered rings and is the NH-racemate while the macrocyclic subunit in $[Ni_2L^3]$ having a $\delta\lambda$ set of lateral metallorings is the NH-*meso* isomer.¹¹

Both $[NiL^1]$ and $[NiL^2]$ are highly hydrated solids and hydrogen bonds play an important role in the stabilisation of crystal lattices (Fig. 2 and Supplementary Table S2). At the same time, no water molecules are co-ordinated and the complexes remain diamagnetic both in the solid state and in aqueous solution (see below).

The crystal lattice of $[NiL^1]\cdot 6H_2O$ has a layered form with columnar arrangement of macrocyclic units along the *a* axis (Fig. 2). The interlayer interaction is realised through direct hydrogen bonds between macrocyclic carbonyl oxygen atoms and the secondary amino group (Table S2). All water molecules in $[NiL^1]\cdot 6H_2O$, except $H_2O(3)$, are located in the intercolumnar space linking both the layers in a column and the columns in a lattice with the formation of fused 4- and 9-membered oxygen rings. Water molecule $H_2O(3)$ is located between the

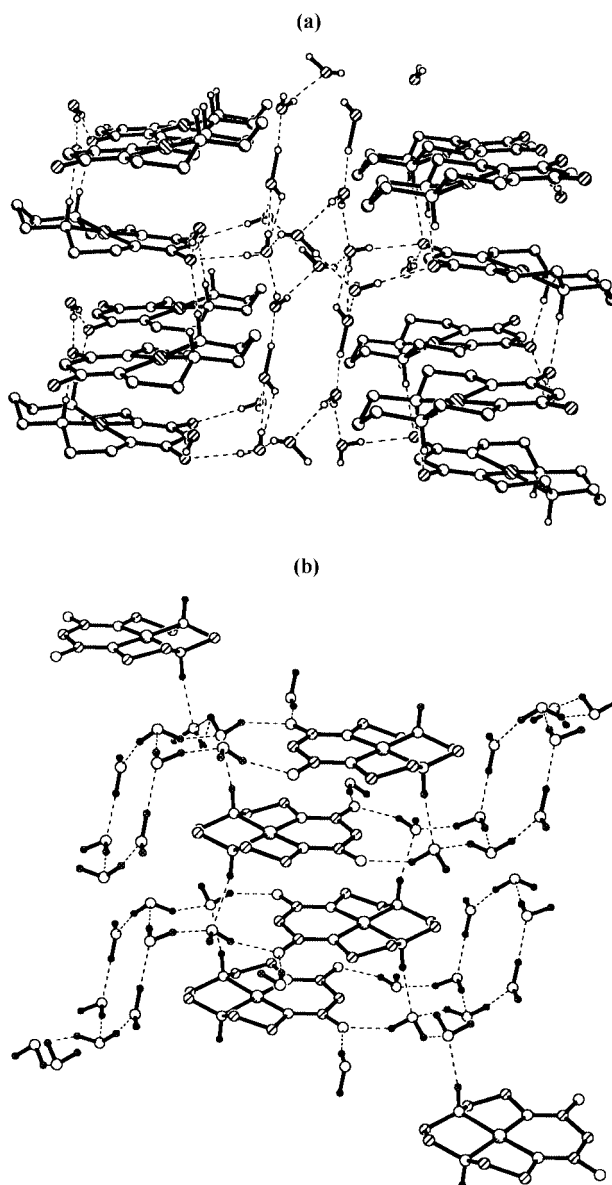


Fig. 2 Fragments of the crystal lattice of $[NiL^1]\cdot 6H_2O$ (a) and $[NiL^2]\cdot 5H_2O$ (b) showing the arrangement of macrocyclic units bridged through hydrogen bonds (dashed lines).

carbonyl oxygen atoms O(1) and O'(2) of the two macrocycles just below the nickel ion of another layer at a distance (2.957 Å) which is too long to be considered as a co-ordination bond.

The macrocyclic units in the crystal lattice of $[NiL^2]\cdot 5H_2O$ form zigzag columns along the *c* axis with the alternating molecules rotated by 180° (Fig. 2). There are no direct hydrogen bonds between macrocycles and they are held together by two bridging water molecules. The main role in gluing the molecules in the *ab* plane is played by the 6-membered oxygen rings each of which binds together four macrocyclic units.

¹H NMR spectra and conformations of the complexes in aqueous solution

NMR investigations of amine macrocyclic nickel(II) complexes in aqueous solution are usually complicated by the line broadening caused by the presence of the paramagnetic 6-co-ordinated form equilibrated with the low spin 4-co-ordinated complex. Previous studies have been limited to a few specific examples including the nickel(II) complexes of unsubstituted 13- and 14-membered tetraamines²⁰ or their hexamethyl substituted derivatives.²¹ In contrast to polyamines, nickel(II) complexes with amide containing macrocycles are diamagnetic and

Table 4 Proton chemical shifts δ (ppm) and geminal coupling constants J /Hz for nickel(II) macrocyclic complexes obtained by simulation of ^1H NMR spectra (for labelling see Fig. 3 and 5)

NiL ¹			N- <i>rac</i> [NiL ²]			N- <i>meso</i> [NiL ²]		
H	δ	J	H	δ	J	H	δ	J
Malonamide ring								
<i>i</i>	2.988	−20.4	<i>i</i>	3.100	—	<i>i</i>	2.963	−20.8
<i>j</i>	3.241		<i>j</i>	3.100		<i>j</i>	3.243	
Lateral 5-membered rings								
<i>e</i>	2.357	−11.4	<i>e</i>	2.879	−11.1	<i>e</i>	3.147	−11.3
<i>f</i>	2.505		<i>f</i>	2.638		<i>f</i>	2.694	
<i>g</i>	2.578	−13.6	<i>g</i>	2.829	−13.8	<i>g</i>	2.749	−13.7
<i>h</i>	3.146		<i>h</i>	3.431		<i>h</i>	3.366	
6-Membered ring			Central 5-membered ring					
<i>a</i>	1.299	−15.8	<i>k</i>	2.724	−12.6	<i>k</i>	2.850	−12.9
<i>b</i>	1.876		<i>l</i>	2.872		<i>l</i>	3.276	
<i>c</i>	2.555	−12.3						
<i>d</i>	2.502							

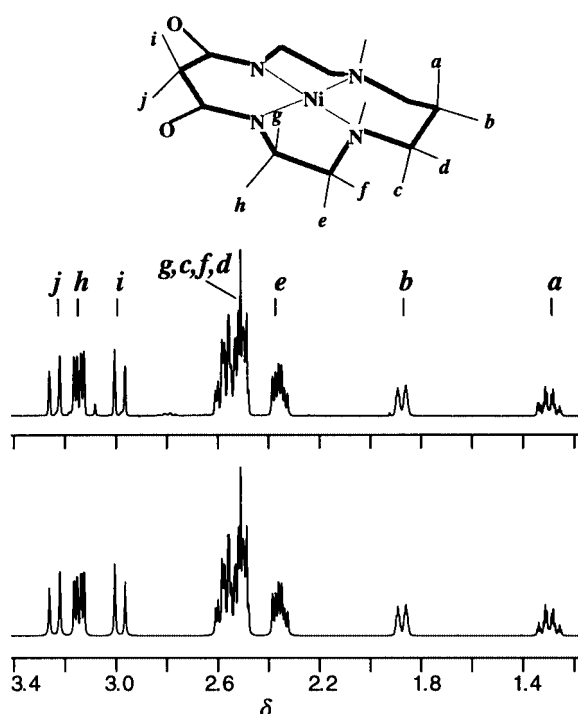


Fig. 3 Experimental (top) and simulated (bottom) ^1H NMR spectra of $[\text{NiL}^1]$.

hence provide an excellent opportunity for NMR studies of these species in solution.

Typically, ^1H NMR spectra of the azamacrocyclic transition metal complexes are complicated due to the “frozen” conformations of chelate rings and the spectra of $[\text{NiL}^1]$ and $[\text{NiL}^2]$ (Figs. 3 and 4) are no exception. Conformational rigidity of such systems results from the fact that the inversion of the chelate rings requires a change of the configuration of coordinated amine nitrogen atom(s). This process proceeds *via* deprotonation and occurs at appreciable rate only under strongly basic conditions.²² In the absence of structural restriction, as for the open chain complex $[\text{NiL}^4]$, the rings are inverting rapidly and this compound reveals a simple averaged spectrum showing a singlet at δ 3.11 (malonamide CH_2 group) and two triplets at δ 2.42 and 2.86 (CH_2 groups of chelate rings).²³

The spectrum of $[\text{NiL}^1]$ (Fig. 3) consists of a number of non-overlapping multiplets (number of protons in parentheses, for labelling see Fig. 3): *a* (1), *b* (1), *e* (2), *h* (2), *i* (1) and *j* (1),

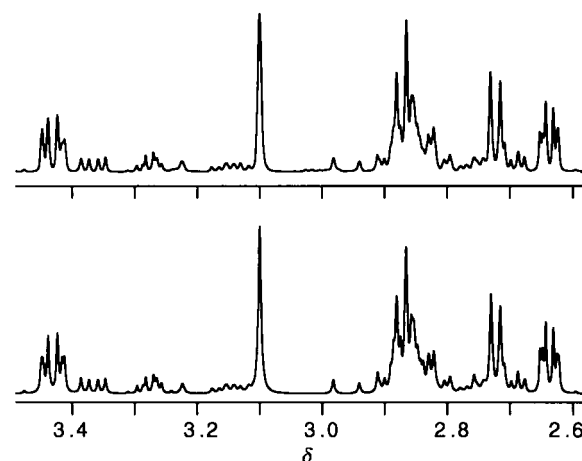


Fig. 4 Experimental ^1H NMR spectrum of $[\text{NiL}^2]$ (top) and spectrum simulated for a mixture of *N-rac* (80%) and *N-meso* (20%) isomers (bottom).

and a complex pattern in the region δ 2.47–2.62 integrating to 8 protons. The signals of the central methylene groups in both 6-membered chelate rings can readily be identified based on their chemical shifts and coupling constants. The multiplets in the high-field region are characteristic of the trimethylenediamine ring in a chair conformation (axial and equatorial protons, *a* and *b*, respectively).²⁰ The pair of protons from the malonamide fragment (*i*, *j*) appears as an AB-type subspectrum centered at δ 3.115 with $J(\text{H}^i\text{H}^j)$ of 20.3 Hz.

The 2-D correlation spectrum of $[\text{NiL}^1]$ (Supplementary) reveals that a complex pattern in the region δ 2.47–2.62 is the superposition of signals (*c*, *d*, *f*, *g*) belonging to two spin systems of the 6- and 5-membered chelate rings. The observation of the cross-peaks in the 2-D spectrum due to long-range coupling (5J) between malonamide protons and protons *g* and *h* allows unambiguous assignment of the latter to the CH_2 group attached to the amide nitrogen. Further analysis was performed by computer simulation of the subspectra of 5- and 6-membered rings and the resulting parameters giving reasonable agreement with the experimental spectrum (Fig. 3) are collected in Tables 4 and 5.

The spectrum of $[\text{NiL}^2]$ (Fig. 4) is quite different from that of the 14-membered analogue. In addition, along with the main signals it contains a number of peaks of considerably lower intensity, which do not disappear on repeated recrystallisation of the complex. It was concluded based on the analysis of the spectrum (see below) that $[\text{NiL}^2]$ is actually a mixture of NH-

Table 5 H–C–C–H dihedral angles φ ^a and calculated^b and experimental^c vicinal constants (Hz) for nickel(II) macrocyclic complexes (for labelling see Figs. 3 and 5)

H	φ	$J_{\text{calc}}(1)$	$J_{\text{calc}}(2)$	J_{exp}	H	φ	$J_{\text{calc}}(1)$	$J_{\text{calc}}(2)$	J_{exp}
[NiL¹]									
Lateral 5-membered rings					6-Membered ring				
<i>e</i> – <i>g</i>	160.3	11.8	11.4	12.5	<i>a</i> – <i>c</i>	171.3	12.8	12.2	12.9
<i>e</i> – <i>h</i>	39.7	7.2	6.3	6.2	<i>a</i> – <i>d</i>	69.5	2.9	1.9	2.9
<i>f</i> – <i>g</i>	40.1	7.1	6.2	5.1	<i>b</i> – <i>c</i>	69.2	2.9	1.4	2.3
<i>f</i> – <i>h</i>	80.6	2.1	0.5	1.6	<i>b</i> – <i>d</i>	49.9	5.5	4.1	3.6
N-<i>rac</i>[NiL²]									
Lateral 5-membered rings					Central 5-membered ring				
<i>e</i> – <i>g</i>	159.6	11.7	11.3	12.9	<i>k</i> – <i>k'</i>	170.3	12.7	12.0	13.8
<i>e</i> – <i>h</i>	38.9	7.3	6.4	6.4	<i>l</i> – <i>l'</i>	71.4	2.7	0.9	0.6
<i>f</i> – <i>g</i>	38.9	7.3	6.4	5.1	<i>k</i> – <i>l'</i>	49.6	5.6	4.6	4.8
<i>f</i> – <i>h</i>	81.8	2.1	0.5	0.3	<i>l</i> – <i>k'</i>	49.3	5.6	4.6	4.8
N-<i>meso</i>[NiL²]									
Lateral 5-membered rings					Central 5-membered ring				
<i>e</i> – <i>g</i>	161.2	11.9	11.4	12.8	<i>k</i> – <i>k'</i>	45.7	6.2	5.2	5.9
<i>e</i> – <i>h</i>	40.5	7.0	6.1	6.2	<i>l</i> – <i>l'</i>	45.1	6.3	5.3	5.9
<i>f</i> – <i>g</i>	40.6	7.0	6.1	5.5	<i>k</i> – <i>l'</i>	165.7	12.4	11.8	
<i>f</i> – <i>h</i>	80.1	2.1	0.5	0.4	<i>l</i> – <i>k'</i>	75.0	2.4	0.7	
					$\frac{1}{2}[J(\text{H}^k\text{H}^{l'}) + J(\text{H}^{l'}\text{H}^{k'})]$		7.4	6.2	6.8

^a Taken from structural data; averaged values when two pairs of protons are present. ^b $J_{\text{calc}}(1) = 5\cos(2\varphi) - \cos\varphi + 7$; $J_{\text{calc}}(2)$ calculated according to ref. 24 with parameter set A. ^c Obtained by simulation of ¹H NMR spectra.

rac (as in the solid state) and NH-*meso* isomers. The possibility of the existence of the second isomer seems quite reasonable bearing in mind that the macrocyclic subunit in the parent [Ni₂L³] has just the *meso* configuration of NH centres.¹¹

The spectrum of the major compound consists of a singlet at δ 3.100 assigned to malonamide protons *i* and *j* (for labelling see Fig. 5), two multiplets in the high-(*f*) and low-field (*h*) regions, a doublet-like multiplet at δ 2.72 (*k*) and a complex pattern at δ 2.79–2.82. According to the 2-D correlation spectrum (Supplementary) there are two different spin systems in this spectrum. The first one can be recognised as an AA'BB' spin system of the central 5-membered chelate ring and includes multiplet *k* and its symmetric counterpart *l* located in the overlapping region. The second four-spin system includes four protons (*e*, *f*, *g*, *h*) of the lateral 5-membered rings.

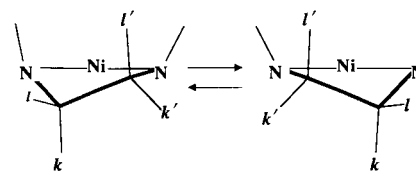
The spectrum assigned to the minor component of [NiL²] consists of the signals of three separate spin systems: the methylene group of malonamide (AB system), central 5-membered chelate ring (AA'BB' system) and lateral 5-membered chelate rings (4 non-equivalent protons). As for [NiL¹], both isomers of [NiL²] exhibit additional cross-peaks between the malonamide CH₂ group and two protons (*g*, *h*) adjacent to amide nitrogen atoms in the 2-D correlation spectrum. Chemical shifts and coupling constants obtained by simulation of the spectra (Fig. 5) are presented in Tables 4 and 5.

Based on integration, the relative amounts of the major and minor forms of [NiL²] in solution can be estimated to be *ca.* 4:1. As can be seen from Fig. 4, the weighted sum of the simulated spectra of both these compounds reproduces the experimental spectrum reasonably well.

Since all the complexes under consideration contain a common structural fragment it was of interest to compare their NMR parameters and to check whether these parameters are compatible with the solid state geometry. The most direct structural information is provided by the values of vicinal coupling constants which can be correlated to H–C–C–H dihedral angles through Karplus-type equations (Table 5). As can be seen, in all cases, except for the central 5-membered ring in the minor form

of [NiL²], a reasonable agreement between experimental and calculated values of ³*J* is observed supporting that the structure of complexes in solution is basically the same as in the solid state. However, the limited precision of the Karplus equation does not allow more definite conclusions. The general trend with a commonly used form of the equation ($J_{\text{calc}}(1)$) is an underestimation of the largest (*trans*) and an overestimation of the other constants. The employment of the generalised relationship taking into account electronegativity and orientation of substituents²⁴ [$J_{\text{calc}}(2)$] makes *trans* constants worse but in most cases improves the agreement for constants corresponding to smaller dihedral angles. (It should be mentioned that the assignment of correct electronegativities to co-ordinated amino and amide groups is a serious problem and in our calculations both the differences between these nitrogen atoms and the effect of the metal ion were completely neglected.)

The situation with vicinal constants for the central 5-membered chelate ring of the NH-*meso* isomer of [NiL²] needs special comments. In this case the large $J(\text{H}^k\text{H}^{l'})$ and the small $J(\text{H}^{l'}\text{H}^k)$ constants calculated for a fixed ring conformation (based on the solid state structure of [Ni₂L³]) are not observed. At the same time, the experimental value of 6.8 Hz is rather close to the average of their calculated values. In our opinion, this feature can be explained by a rapid exchange between two enantiomeric conformations of this ring (Scheme 1). Such a



Scheme 1

process does not require a change of configuration of NH centres and hence can be expected to be fast on the NMR timescale.

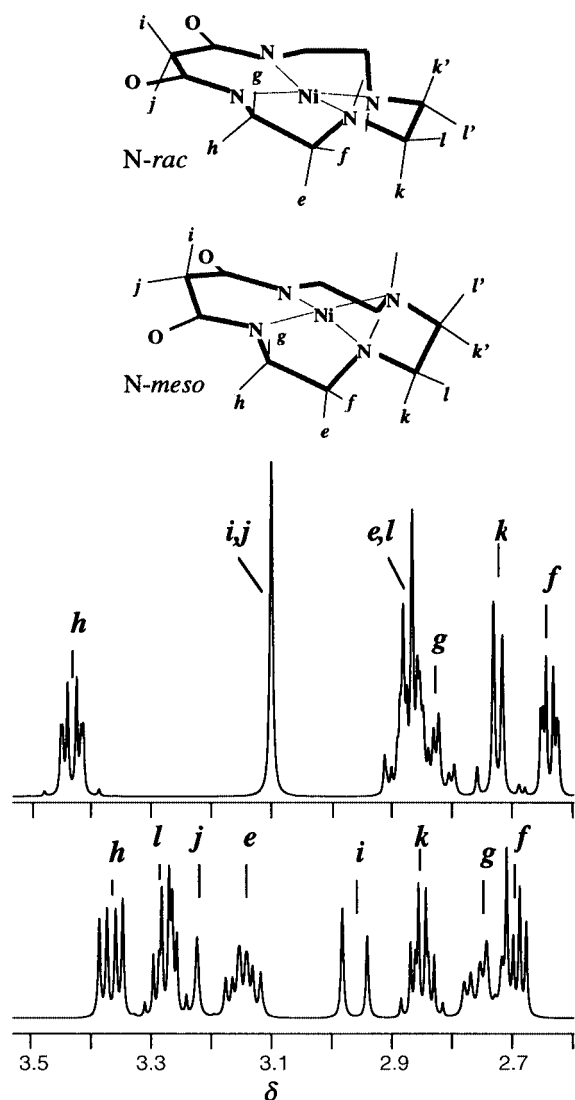


Fig. 5 Simulated ^1H NMR spectra of N-*rac* (top) and N-*meso* (bottom) isomers of $[\text{NiL}^2]$.

As one can conclude based on the data of Tables 4 and 5, a quite different appearance of the subspectra of the lateral 5-membered rings in the compounds under study is due to the considerable variations of chemical shifts but not of coupling constants. Though the values of δ show no characteristic behaviour some trends in their variations can be mentioned. In all cases the proton *h* is most deshielded and the relative order of chemical shifts is $\delta_h \gg \delta_g > \delta_f$. The shift of H^e is most sensitive to the structure of the ligand. It should also be noted that the subspectra of these rings for $[\text{NiL}^2]$ are considerably shifted downfield as compared to the complexes of 14-membered and open chain ligands.

In the complex $[\text{NiL}^1]$ the axial proton (*c*) of the trimethylenediamine chelate ring is slightly deshielded as compared to the equatorial one (*d*) and usually chemical shifts of protons of methylene groups attached to the co-ordinated nitrogen in 6-membered chelate rings are highly sensitive to structural variations.²⁰ On the other hand, those of protons of the remote CH_2 group (*a* and *b*) are much more predictable. In the present case their relative order ($\delta_{\text{ax}} < \delta_{\text{eq}}$) and separation are similar to those of other macrocyclic complexes^{20,21} and 6-membered organic rings.²⁵ The averaged values of the shifts of malonamide protons *i* and *j* are very similar in the whole series: δ 3.12 $[\text{NiL}^1]$, 3.10 (NH-*rac* $[\text{NiL}^2]$), 3.10 (NH-*meso* $[\text{NiL}^2]$), and 3.11 $[\text{NiL}^4]$. It should be noted that these protons are equivalent only for the major (NH-*rac*) isomer of $[\text{NiL}^2]$ in which, according to structural data, this ring is very flattened once again

supporting a similarity of conformations in the solid state and in solution.

One more interesting property of the malonamide-derived macrocyclic complexes is the appearance of long-range (through 5 bonds) coupling between malonamide CH_2 protons and the protons of methylene groups in the lateral chelate rings. In all compounds the signals of H^g revealed additional triplet splitting (resolution enhancement gives the *J* value as ca. 1.4 Hz) while the splitting of H^h is not observable in the 1-D spectrum. Apparently, the relatively large values of 5J are due to the presence of the conjugated amide group.

Conclusion

The crystal structure analysis of the nickel(II) complexes of the 14- and 13-membered malonamide-derived macrocycles $[\text{NiL}^1] \cdot 6\text{H}_2\text{O}$ and $[\text{NiL}^2] \cdot 5\text{H}_2\text{O}$ revealed that in both compounds the metal ion possesses a square planar co-ordination environment formed by two deprotonated amide and two amine groups. The $\text{Ni}-\text{N}_{\text{amide}}$ and $\text{Ni}-\text{N}_{\text{amine}}$ bonds are shorter in the complex of the 13-membered as compared to the 14-membered macrocycle. Water molecules do not co-ordinate but form an extended network of hydrogen bonds. The ligand in the $[\text{NiL}^1] \cdot 6\text{H}_2\text{O}$ has the N-*meso* and in $[\text{NiL}^2] \cdot 5\text{H}_2\text{O}$ the N-*rac* configuration of the secondary amino groups.

Careful analysis of ^1H NMR spectra revealed that the spectrum of $[\text{NiL}^1]$ in solution is compatible with the N-*meso* configuration of NH centres found in the solid state. At the same time, for the complex of the 13-membered macrocycle $[\text{NiL}^2]$ both possible diastereomers, N-*meso* and N-*rac*, are present in solution, with the major component being the N-*rac* isomer found in the crystal structure. The values of spin-spin coupling constants reveal a good reproducibility within the series of compounds and vicinal constants are consistent with the solid state geometry. On the contrary, the values of chemical shifts generally do not demonstrate characteristic behaviour.

Acknowledgements

Generous financial support by the Royal Society of Chemistry and the Department of Basic Research of the Ministry of the Ukraine for Science and Technology is gratefully acknowledged.

References

- 1 D. W. Margerum and G. D. Ovens, in *Metal Ions in Biological Systems*, ed. H. Sigel, Marcel Dekker, New York, 1981, vol. 12, p. 75; J. S. Rybka and D. W. Margerum, *Inorg. Chem.*, 1980, **19**, 2784; *Inorg. Chem.*, 1981, **20**, 1453.
- 2 (a) T. J. Collins, R. D. Powell, C. Slebodnick and E. S. Uffelman, *J. Am. Chem. Soc.*, 1991, **113**, 8419; J. M. Workman, R. D. Powell, A. D. Procyk, T. J. Collins and D. F. Bocian, *Inorg. Chem.*, 1992, **31**, 1548; K. L. Kostka, B. G. Fox, M. P. Hendrick, T. J. Collins, C. E. E. Rickard, L. J. Wright and E. Münck, *J. Am. Chem. Soc.*, 1993, **115**, 6746; (b) T. J. Collins, T. R. Nichols and E. S. Uffelman, *J. Am. Chem. Soc.*, 1991, **113**, 4708; T. J. Collins, K. L. Kostka, E. S. Uffelman and T. L. Weinberger, *Inorg. Chem.*, 1991, **30**, 4204.
- 3 (a) E. Kimura, *J. Coord. Chem.*, 1986, **15**, 1; *Pure Appl. Chem.*, 1986, **58**, 1461; *Crown Compounds Toward Future Application*, ed. S. R. Cooper, VCH, New York, 1992, ch. 6; (b) X. H. Bu, X. C. Cao, D. L. An, R. H. Zhang, T. Clifford and E. Kimura, *J. Chem. Soc., Dalton Trans.*, 1998, 433; X. H. Bu, D. L. An, X. C. Cao, R. H. Zhang, T. Clifford and E. Kimura, *J. Chem. Soc., Dalton Trans.*, 1998, 2247; (c) E. Kimura, Y. Lin, R. Machida and H. Zenda, *J. Chem. Soc., Chem. Commun.*, 1986, 1020; E. Kimura, S. Korenari, M. Shionoya and M. Shiro, *J. Chem. Soc., Chem. Commun.*, 1988, 1166.
- 4 L. Fabbri, *Comments Inorg. Chem.*, 1985, **4**, 33; G. De Santis, L. Fabbri, M. Licchelli and P. Pallavicini, *Coord. Chem. Rev.*, 1992, **120**, 237; L. Fabbri, T. A. Kaden, A. Perotti, B. Seghi and L. Siegfried, *Inorg. Chem.*, 1986, **25**, 321; T. R. Wagner and C. J. Burrows, *Tetrahedron Lett.*, 1988, **29**, 5091; T. R. Wagner, Y. Fang and C. J. Burrows, *J. Org. Chem.*, 1989, **54**, 1584.

- 5 R. W. Hay and P. R. Norman, *Transition Met. Chem.*, 1980, **5**, 232; R. W. Hay, R. Bembi and W. Sommerville, *Inorg. Chim. Acta*, 1982, **59**, 147; R. W. Hay, M. P. Pujari and F. McLaren, *Inorg. Chem.*, 1984, **23**, 3033; R. W. Hay and M. M. Hassan, *Transition Met. Chem.*, 1994, **19**, 129; L. C. Siegfried and T. A. Kaden, *J. Phys. Org. Chem.*, 1992, **5**, 549; A. Marchi, R. Rossi, L. Magon, A. Duatti, U. Casellato, R. Graciani, M. Vidal and F. Riche, *J. Chem. Soc., Dalton Trans.*, 1990, 1935.
- 6 M. Kodama and E. Kimura, *J. Chem. Soc., Dalton Trans.*, 1981, 694.
- 7 Ya. D. Lampeka and S. P. Gavrish, *J. Coord. Chem.*, 1990, **21**, 351; S. P. Gavrish and Ya. D. Lampeka, *J. Coord. Chem.*, 1991, **24**, 351; *Russ. J. Inorg. Chem.*, 1993, **38**, 1211; *J. Coord. Chem.*, 1996, **38**, 295; *Russ. J. Inorg. Chem.*, 1997, **42**, 660.
- 8 I. Tabushi, H. Okino and Y. Kuroda, *Tetrahedron Lett.*, 1976, 4339; I. Tabushi, Y. Taniguchi and H. Kato, *Tetrahedron Lett.*, 1977, 1049.
- 9 M. Kodama and E. Kimura, *J. Chem. Soc., Dalton Trans.*, 1979, 325.
- 10 (a) H. B. Xian, L. A. Dao, A. Z. Zhi, T. C. Yun, M. Shionoya and E. Kimura, *Polyhedron*, 1997, **16**, 179; X. H. Bu, X. C. Cao, Z. H. Zhang, Z. A. Zhu, Y. T. Chen, M. Shionoya and E. Kimura, *Polyhedron*, 1996, **15**, 1203; (b) P. Chinn, D. H. Busch and N. W. Alcock, *Acta Crystallogr., Sect. C*, 1993, **49**, 1284; J. K. Moran, M. M. Olmstead and C. P. Meares, *Acta Crystallogr., Sect. C*, 1995, **51**, 621; E. Kimura, M. Sasada, M. Shionoya, T. Koike, H. Karosaki and M. Shiro, *J. Biol. Inorg. Chem. (JBIC)*, 1997, **2**, 74.
- 11 P. Comba, S. P. Gavrish, R. W. Hay, P. Hilfenhaus, Ya. D. Lampeka, P. Lightfoot and A. Peters, *Inorg. Chem.*, 1999, **38**, 1416.
- 12 R. M. Lewis, G. H. Nancollas and P. Coppens, *Inorg. Chem.*, 1972, **11**, 1371.
- 13 L. Fabbrizzi, A. Poggi and B. Seghi, *Inorg. Synth.*, 1985, **23**, 83; L. Fabbrizzi, A. Perotti and A. Poggi, *Inorg. Chem.*, 1983, **22**, 1411.
- 14 A. Altomare, M. C. Burla, M. Camali, M. Cascarano, M. Giacobazzo, A. Guagliardi and A. Polidori, *J. Appl. Crystallogr.*, 1993, **26**, 343.
- 15 TEXSAN: Crystal Structure Analysis Package, Molecular Structure Corporation, The Woodlands, TX, 1995.
- 16 P. H. M. Budzelaar, gNMR, Ivory Soft, Cherwell Scientific Publishers, Oxford, 1996.
- 17 J. Macicek, G. Gencheva, M. Miteva, P. R. Bontchev, Ya. D. Lampeka and S. P. Gavrish, *J. Inclusion Phenom.*, 1992, **13**, 195.
- 18 Z. Zhang, J. L. Petersen and A. M. Stolzenberg, *Inorg. Chem.*, 1996, **35**, 4649.
- 19 S. Zhu, Q. Luo, M. Shen and L. Huang, *Acta Crystallogr., Sect. C*, 1992, **48**, 1926.
- 20 E. J. Billo, P. J. Connolly, D. J. Sardella, J. P. Jasinski and R. J. Butcher, *Inorg. Chim. Acta*, 1995, **230**, 19.
- 21 J.-W. Chen, C.-C. Chang and C.-S. Chung, *Inorg. Chem.*, 1986, **25**, 4794.
- 22 E. Sledziewska, *Bull. Acad. Sci. Pol., Ser. Sci. Chim.*, 1972, **20**, 49; P. J. Connolly and E. J. Billo, *Inorg. Chem.*, 1987, **26**, 3224.
- 23 H. A. O. Hill and K. A. Rospin, *J. Chem. Soc. A*, 1968, 3036.
- 24 C. A. G. Haasnoot, F. A. A. M. de Leeuw and C. Altona, *Tetrahedron*, 1980, **36**, 2783.
- 25 H. Günther, *NMR Spectroscopy. An Introduction*, Wiley, Chichester, 1980.